

KINETIC AND ADSORPTION EQUILIBRIUM STUDIES FOR REMOVAL OF TEXTILE DYE FROM AQUEOUS SOLUTIONS ON NUT SHELL ADSORBENT

L Aidani Ykhlef,^{*} Henini Ghania^{*} and Hanini Salah^{**}

^{*}Chlef University, Hay Essalem, P.O. Box 151, 02000 Chlef, Algeria

^{**}Medea University, LBMPT, Urban Pole, 26000 Medea, Algeria

✉ Corresponding author: Y. Laidani, l.ykhlef@gmail.com

Received April 13, 2024

In the present work, the objective has been to determine the potential of a natural residue material, namely, nut shells, for the removal of Methylene blue dye from aqueous solutions. Adsorption studies were carried out varying parameters, such as contact time, pH, initial concentration and temperature, in order to find the optimum ones. The results obtained showed that the nut shell adsorbent had an adsorption capacity of 16.44 mg/g for Methylene blue. The adsorption process was rapid and reached equilibrium in 20 min of contact at 45 °C and pH 6. Different adsorption models, namely, the Langmuir, Freundlich, Temkin and Elovich ones, were examined for the description of the adsorption data, and it was found that the best fit of experimental data was achieved by the Langmuir model. Also, the pseudo-first-order and pseudo-second-order kinetic models were applied to the experimental data. The experimental data fitted very well the pseudo-second-order kinetic model and followed the model of intraparticle diffusion (K_{dif} varied from 1.694 to 3.584 mg/(g min^{1/2}) for concentrations between 30 and 70 mg/L, whereas diffusion was not the only rate-limiting step. The adsorption using the studied system (nut shells/Methylene blue) proved to be an exothermic and spontaneous process. The biosorbent was characterized by various techniques, including FT-IR and XRD.

Keywords: nut shells, Methylene blue dye, adsorption, modeling, kinetics

INTRODUCTION

Water is a vital resource for life and its scarcity on a planetary level is an alarming issue. In this context, pollution of existing water resources gives rise to increasing concerns. Most industrial effluents are loaded with contaminating agents that may cause environmental pollution. Among industrial effluents, colored effluents produced by large industrial activities, such as dyeing of leather, textiles, paper, plastics, as well as by the cosmetic, food and pharmaceutical industries,¹ are considered a threat to ecosystems.

Dyes represent the reference model of persistent organic pollutants discharged into industrial waters.²⁻⁵ Moreover, these compounds are difficult to biodegrade and many of them are toxic, mutagenic and carcinogenic, causing disorders in the digestive, reproductive and nervous systems, as well as liver function, of living organisms.² Methylene blue is a basic blue dyestuff, with the chemical formula C₁₆H₁₈N₃SCl. In spite of not being strongly hazardous, methylene blue can produce harmful effects, when ingested, inhaled or upon skin contact; it

can cause severe eye irritation.⁶ Moreover, it can disturb ecosystems by hindering light penetration.

Several wastewater treatment methods have been investigated, among them, coagulation and flocculation, electro-flocculation, membrane filtration, advanced oxidation, ozonation, ion exchange, reverse osmosis, biodegradation, electrochemical methods, electrocoagulation and adsorption. Of these, adsorption is a technique for removing dyes and other pollutants from aqueous solutions, based on the property of adsorbents to accumulate those pollutants through mechanisms, such as physical adsorption, complexing and ion exchange. The most commonly used natural biosorbents are totally renewable, their cost is low and their use and handling involve no additional risks; they may also be specifically selective for certain pollutants and are generally disposed of by incineration.⁷ Also, while most of the mentioned water treatment methods require high costs and are difficult to operate, particularly on a large scale, adsorption has attracted increasing interest owing to its lower cost and ease of operation.⁸⁻¹⁰

Many natural biomass materials, such as spent coffee grounds,¹¹ Brasil nut shells,¹² garlic peel,¹³ banana stalk waste,¹⁴ soybean hulls,¹⁵ peanut hulls,¹⁶ mango seeds,¹⁷ yellow passion fruit waste,¹⁸ wheat straw,¹⁹ potato plant wastes²⁰ *etc.*, have been studied for the adsorption of dyes.

Nut shells have been investigated in this work as a potential adsorbent of pollutants from aqueous medium, due to the presence in their structure of large numbers of functional groups attached to cell walls, with high binding ability, as well as due to the natural abundance of nut trees around the world. In this study, nut shells were used as an alternative biosorbent for removing methylene blue dye from aqueous solutions. The sorption capacity of nut shells for methylene blue was investigated under the effect of varying pH of the solution, adsorbent dose, initial concentration of the dye, contact time, and temperature. Also, the nut shell adsorbent was characterized before and after adsorption using Fourier transform infrared spectroscopy and X-ray diffraction.

EXPERIMENTAL

Preparation of adsorbent

Nut shells of *Juglans regia* were collected in the north of Algeria and used as adsorbent in this study. Nut shells were washed with distilled boiling water for

15 min, then were placed in a solution of NaOH (12%) for 15 min, washed again with tap water and finally dried for 24 hours. Then, the shells were treated with 12% sodium hypochlorite for 90 min at ambient temperature, after which they were rinsed with distilled water several times. The nut shells (NS) were oven dried at 60 °C for 24 hours, then crushed and sifted. The obtained samples were considered ready for the adsorption study.

Preparation of adsorbate

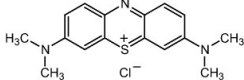
Methylene blue (MB) dye has the chemical formula: C₁₆H₁₈ClN₃S, is cationic, its solubility in water is of 1 g/L, with the maximum absorption wavelength λ_{\max} = 664 nm. Methylene blue (MB) dye was purchased from Sigma Aldrich. Its characteristics are summarized in Table 1. Stock solutions of the dye were prepared by dissolving precise amounts of the dye in distilled water to give a concentration of 1 g/L. The initial pH of the dye solution was adjusted by adding a dilute solution of 0.1N HCl or 0.1N NaOH, and determined using a pH-meter (AD1030 Professional pH-ORP-TEMP Bench Meter, Romania).

Physical properties of the material

Particle size measurement

The particle size of the samples was determined by using a certain number of sieves of different mesh sizes of the Retsch brand (type AS200).²¹

Table 1
Properties and characteristics of MB dye

Chemical name (IUPAC)	Dimethylamino-3,7 phenazathionium chloride
Molecular weight (g/mol)	373.90
Molecular volume (cm ³ /mol)	241.9
Molecular diameter (nm)	0.8
Chemical structure	

Moisture content

The moisture content is a ratio expressed as a percentage, it is determined by drying the adsorbent in an oven at 105 °C until its weight remains constant. It is then calculated by the following relationship:²²

$$H(\%) = \frac{(W_0 - W_d)}{W_0} 100 \quad (1)$$

where H is the moisture as a percentage of weight (%), W₀ initial weight of the sample (before drying) and W_d is the dry weight of the sample (after drying).

Ash content

In order to determine the content of mineral matter in the adsorbent, 1 g of dry adsorbent was weighed and

placed in a calcination crucible, then introduced into an oven at 600 °C for 45 min. After cooling, the crucible was weighed again. The ash content was determined by the following relation:²³

$$C(\%) = \frac{P_2}{P_1} 100 \quad (2)$$

where P₁ – the weight of the dry adsorbent placed in the crucible, and P₂ – the weight of the ash in the crucible.

Apparent density

To measure the apparent volumetric weight (g/cm³) of the grains making up a solid, a pycnometer is most often used (BRAND™ 43338), which is a glass container fitted with a ground capillary tube stopper.

After having precisely determined the internal volume V of the pycnometer, the empty pycnometer W_1 was weighed, then a dry sample weight was introduced into the pycnometer (W_2), finally the pycnometer was filled with water of known volumetric weight (ρ_{eau}) taking care to release all air bubbles. The weight of the pycnometer filled with the sample and water was then noted as W_3 . The apparent density of the sample was calculated using the following formula:²⁴

$$\rho_{app} = \frac{W_2 - W_1}{V - \frac{W_3 - W_2}{\rho_{eau}}} \quad (3)$$

External porosity

In order to determine external porosity, a certain quantity of adsorbent was weighed, introduced into a test tube of volume V_1 , then filled with water (V_2) and W_2 was weighed. The external porosity was calculated by the following relation:²⁵

$$\varepsilon_{ext} = \frac{(\rho_{eau} - W_2) - V_1}{V_T} \quad (4)$$

where ε_{ext} is the external porosity; $\varepsilon = 0.3966$; W_1 the weight of the adsorbent (g) and W_2 is the weight of water (g), V_1 volume of the adsorbent occupied in the test tube (cm^3), V_T is the total volume ($V_T = V_1 + V_2$) (cm^3) and ρ_{eau} is the density of water (g/cm^3).

Water swelling

The swelling degree of the adsorbent corresponds to the increase in volume of a known weight of biosorbent placed in contact with distilled water. Its determination was carried out by measuring the volume occupied in a 100 mL test tube by a known weight of dry material (1 g). After adding distilled water, the suspension was homogenized and left to stand at room temperature for 24 hours. Water swelling was expressed as the ratio of the volume of hydrated sample to that of the dry sample.²⁶

Characterization techniques

The nut shells (NS) were characterized before and after adsorption by Fourier transform infrared spectroscopy, using a Prestige-21 FTIR, Shimadzu, Japan. The spectra were recorded by scanning from 400 to 4000 cm^{-1} . X-ray diffraction (XRD) analyses were carried out using an APD 2000 model with $\text{Cu-K}\alpha$ irradiation ($\lambda = 1.540598 \text{ \AA}$).

The percentage of crystallinity (X_C (%)) and crystallinity index (C.I.) were calculated as follows:²¹⁻²²

$$X_C(\%) = \frac{I_C}{I_C + I_A} \cdot 100 \quad (5)$$

$$C.I. = \frac{I_C - I_A}{I_C} \quad (6)$$

where I_C is the peak intensity of the crystalline phase, I_A is the peak intensity of the amorphous phase.

Adsorption experiments

Adsorption studies for the evaluation of the NS adsorbent for the removal of MB from aqueous solutions were carried out using batch adsorption experiments. For these experiments, a fixed quantity of adsorbent (1 g) was placed in 500 mL glass Erlenmeyer flasks containing 250 mL of MB solutions of 30, 50 and 70 mg/L MB concentrations, which were agitated for a suitable time (60 min) from 23° to 45 °C at pH 6. After a given contact time (t) corresponding to equilibrium, we recovered the filtrate solution and analyzed it using a UV-visible spectrophotometer (Unicam 8625, LabExchange, France) at 664 nm. Adsorption kinetic experiments were used to investigate the effect of contact time and determine the kinetic parameters. For these tests, 1 g of NS was added to 250 mL MB solutions with different initial concentrations. The mixture was agitated on an electromagnetic stirrer (Shinko Electric CO. LTD, Japan) at 350 rpm. At predetermined time intervals, 10 mL samples were taken out, filtered and spectrophotometer-based analyzed. The same methods were used to determine the residual MB concentration. Each measurement of dye concentration was repeated three times.

The amount of MB adsorbed by the nut shell adsorbent, q_t (mg/g), was calculated by using the following Equation (7):²³⁻²⁴

$$q_t = \frac{(C_0 - C_t)V}{m} \quad (7)$$

where q_t is the amount of MB taken up by the adsorbent (mg/g), C_t (mg/L) is the concentration of MB solution at t time (min), C_0 (mg/L) is the initial concentration of MB dye, V is the volume of dye solution (L), and m is the weight of adsorbent used (g).

Adsorption isotherms

Adsorption isotherms were calculated based on the well-known Langmuir, Freundlich, Temkin and Elovich isotherm models. The Langmuir isotherm assumes monolayer adsorption onto a surface containing a finite number of adsorption sites, using uniform strategies of adsorption.²⁵ The linear form of the Langmuir isotherm equation is given as:

$$\frac{1}{q_e} = \frac{1}{q_m} + \frac{1}{K_L q_m C_e} \quad (8)$$

where C_e is the equilibrium concentration of the adsorbate (mg/L), q_e is the adsorption capacity of adsorbent at equilibrium (mg/g), q_m and K_L are the maximum Methylene blue adsorbed per unit mass of the adsorbent (mg/g) and Langmuir constant, in relation to the energy of sorption, which quantitatively indicates the affinity between the adsorbent and Methylene blue dye (L/mg), respectively.

A favourable or unfavourable adsorption system can be determined based on the essential characteristic of the Langmuir model, which can be expressed in terms of the dimensionless constant separation factor

or equilibrium parameter, R_L , which is defined as follows:

$$R_L = \frac{1}{1 + K_L C_0} \quad (9)$$

where K_L is the Langmuir constant and C_0 is the initial dye concentration. The value of the separation factor indicates the nature of the adsorption process, which can be irreversible ($R_L = 0$), favourable ($0 < R_L < 1$), linear ($R_L = 1$), or unfavourable ($R_L > 1$).⁷⁻²⁶

The adsorption capacity of the biosorbent towards MB dye can be determined using the Freundlich model too. The model describes adsorption as occurring on a heterogeneous surface, and is commonly described by the following equation:²⁷

$$q_e = K_F C_e^{1/n_F} \quad (10)$$

where q_e is the adsorption capacity of adsorbent at equilibrium (mg/g), K_F (mg⁽¹⁻ⁿ⁾.Lⁿ/g) is related to the adsorption capacity, and $1/n_F$ gives an idea about the adsorption affinity and heterogeneity of the adsorbent surface. When $1/n_F$ is small, the adsorption affinity increases, while when $1/n$ is high the heterogeneity of the adsorbent surface is enhanced.²⁸ The equilibrium constants were evaluated from the intercept and the slope, respectively, of the linear plot of $\ln q_e$ versus $\ln C_e$ based on experimental data. The Freundlich equation can be linearized in a logarithmic form for the determination of the constants K_F as follows:²⁹⁻³⁰

$$\ln(q_e) = \ln(K_F) + \frac{1}{n_F} \ln(C_e) \quad (11)$$

Temkin's model rests on the assumption that, during the adsorption phase, the heat of adsorption due to interactions with the adsorbate decreases linearly with the recovery rate θ . From q_e plotted as a function of $\ln C_e$, B_T , and K_T values can be determined:³¹⁻³²

$$q_e = \frac{RT}{B_T} \ln(K_T C_e) \quad (12)$$

where R is the universal gas constant (8.314 J/(mol K)), T is the absolute temperature (°C), B_T is the variation in energy of adsorption (J/mol), and K_T is the Temkin constant (L/mg).

The Elovich equation can also be used to describe adsorption, assuming that the actual solid surfaces are energetically heterogeneous, but the equation does not propose any definite mechanism for adsorbate-adsorbent.³³ It has extensively been accepted that the chemisorption process can be described by this semi-empirical equation.³⁴ The linear form of this equation is given by:³⁵

$$q_t = \frac{1}{\beta_{El}} \ln(\alpha_{El} \beta_{El}) + \frac{1}{\beta_{El}} \ln(t) \quad (13)$$

where α_{El} is the initial adsorption rate (mg/g min), and the parameter b_e is related to the extent of surface coverage and activation energy for chemisorption (g/mg). The Elovich coefficients could be computed from the plots q_t vs $\ln(t)$. The initial adsorption rate, and the desorption constant, β_{El} , were calculated from

the intercept and slope of the straight-line plots of q_t against $\ln(t)$.

Kinetic studies

The rate of the adsorption of MB dye onto the NS adsorbent was also studied according to the pseudo-first-order rate expression of Lagergren model.³³ The integrated form of the Lagergren equation is given by:³⁶

$$\text{Log}(q_e - q_t) = \text{Log}q_e - \frac{K_1}{2.303} t \quad (14)$$

where q_e and q_t are the amounts adsorbed at equilibrium and at time, t (mg/g), and k_1 is the rate constant of the pseudo-first-order adsorption (1/min).

The pseudo-second-order kinetic model can be represented in the following form:³⁷⁻³⁸

$$\frac{t}{q_t} = \frac{1}{K_2 q_e^2} + \frac{1}{q_e} t \quad (15)$$

where k_2 is the rate constant of the pseudo-second order adsorption (g/mg min).

The kinetics of adsorption of the adsorbate on the adsorbent was verified at different initial concentrations (30, 50, and 70 mg/L).

Most adsorption reactions take place through a multi-step mechanism comprising (i) external film diffusion, (ii) intraparticle diffusion, and (iii) interaction between adsorbate and active site. Since the first step is excluded by shaking the solution, the rate-determining step is one of the other two steps. Weber and Morris³⁹ described the intraparticle uptake of the adsorption process to be proportional to the half power of time:

$$q_t = K_{dif} t^{1/2} + C \quad (16)$$

where k_{dif} is the rate constant of intraparticle diffusion (mg/g.min^{1/2}).

Adsorption thermodynamics

Temperature dependence of the adsorption process is associated with several thermodynamic parameters. Thermodynamic considerations of a biosorption process are necessary to conclude whether the process is spontaneous or not. The Gibbs free energy change, ΔG° , is an indication of the spontaneity of a chemical reaction. In addition, both enthalpy and entropy factors must be considered to determine the Gibbs free energy of the process. Reactions occur spontaneously at a given temperature if ΔG° is a negative quantity. The value of ΔG° can be determined from the following equation:¹⁹

$$\Delta G^\circ = RT \ln(K_L) \quad (17)$$

where K_L is the adsorption equilibrium constant, R is the gas constant (8.314 J/mol K), and T is the absolute temperature. The relation between ΔG° , ΔH° (enthalpy), and ΔS° (entropy) can be expressed by the following equations:

$$\Delta G^\circ = \Delta H^\circ - T \Delta S^\circ \quad (18)$$

$$\ln(K_L) = \frac{\Delta S^0}{R} - \frac{\Delta H^0}{RT} = \frac{\Delta G^0}{RT} \quad (19)$$

The values of ΔH^0 and ΔS^0 can be determined from the slope and the intercept of the plot of $\ln(K_L)$ vs $(1/T)$, and ΔG^0 values were calculated using Equation (18).

Error functions

Several mathematically rigorous error functions were used in this study to estimate errors and differences between predicted and experimental values. The root mean square error (RMSE) is defined by Equation (20):⁴⁰

$$RMSE = \sqrt{\left(\frac{1}{N-2}\right) \sum_{i=1}^N (q_{e(cal),i} - q_{e(exp),i})^2} \quad (20)$$

where $q_{e(exp)}$ is the experimental value of uptake, $q_{e(cal)}$ the calculated value of uptake using the model, and N the number of observations in the experiment (the number of data points). The smaller the RMSE values are, the better the curve is fitting.

The sum of error squares (SSE %) is another method that tests the validity of the adsorption models used. The SSE is given by Equation (21):

$$SSE = \frac{1}{N} \sqrt{\sum_{i=1}^N (q_{e(cal),i} - q_{e(exp),i})^2} \quad (21)$$

A low value indicates better SSE smoothing.

Also, the non-linear Chi-square (χ^2) test has been proposed. A low value of Chi-square (χ^2) shows the agreement of experimental data. The Chi-square (χ^2) is determines as follows:

$$\chi^2 = \sum_{i=1}^N \frac{(q_{e(cal),i} - q_{e(exp),i})^2}{q_{e(exp),i}} \quad (22)$$

where the subscripts “*exp*” and “*calc*” show the experimental and calculated values and N is the number of observations in the experimental data. Therefore, in present work both correlation coefficient (R^2) and χ^2 were used to determine the best isotherm model.

RESULTS AND DISCUSSION

Characterization of the adsorbent

The physical characteristics of the material (NS) are shown in Table 2.

FT-IR analysis

FT-IR analysis of the nut shell adsorbent, before and after the adsorption experiment, was performed in the range of 400-4000 cm^{-1} , and the spectra are shown in Figure 1. Both spectra presented a broad band located around 3330 cm^{-1} , which is assigned to O–H stretching vibrations of hydrogen bonded hydroxyl groups. In fact, the hydroxyl groups are present in the primary components of most plant biomass: cellulose, hemicelluloses and lignin.⁴¹

The peak at about 2900 cm^{-1} was attributed to the asymmetric and symmetric stretching vibrations of CH_2 and CH_3 .

Table 2
Physical characteristics of the adsorbent used in the dye adsorption experiments

Characteristics	Values
Particle size (μm)	80
Moisture content (%)	0.10
Ash content (%)	2
Volatile material (%)	90.85
Apparent density (kg/m^3)	11.74
Water swelling (%)	0.63
External porosity	0.396

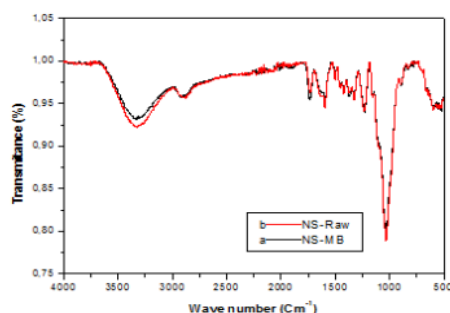


Figure 1: FT-IR spectra of (a) NS-raw and (b) NS loaded MB sample

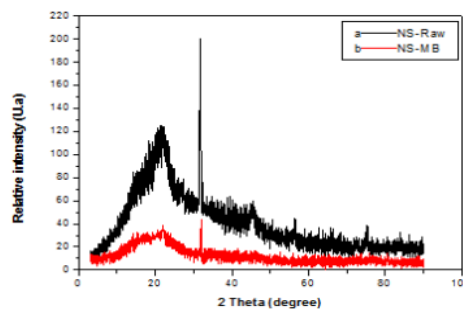


Figure 2: X-ray diffraction patterns of NS before (a) and after (b) adsorption

Table 3
X-ray diffraction results for NS before and after biosorption of MB dye

Sample	2 θ (degree)		Intensity			
	Crystalline peak	Amorphous peak	I _C	I _A	X _C (%)	C.I.
NS raw	31.74	21.6	200	125	61.54	0.37
NS loaded with MB	32.2	21.8	43.4	39	52.67	0.10

The band around 1501 cm⁻¹ was associated with C=C and C=O stretching in the aromatic ring. The peak at 1023 cm⁻¹ may be due to C–O stretching vibrations.⁴² Also, it is important to notice that the band intensities decreased in the FT-IR spectrum of MB loaded NS. This can be explained by the functional groups of the NS surface having been occupied with MB dye, thus confirming the penetration of MB dye into the interlayer space of the NS.

X-ray diffraction studies

The XRD patterns of NS before and after MB adsorption (T = 45 °C, pH = 6, C₀ = 70 mg/L) are shown in Figure 2. Before the adsorption, the NS (raw) showed peaks at 2 θ 31.74° and 21.6°, with relative intensities of 200 and 125, respectively. Also, the NS loaded with MB showed peaks at 32.2° and 21.8°, with relative intensities of 43 and 39, respectively.

The percentage crystallinity of NS raw and NS loaded with MB was determined as 61.54% and 52.67%, and the crystallinity index as 0.37 and 0.10.

It was observed that the intensity of the peak in NS loaded with MB decreased compared to that of the initial adsorbent (Table 3). The decrease in intensity of the peak after the adsorption process indicated decreased crystallinity of the NS loaded with MB. However, the NS loaded with MB also showed broadening of the peak after the adsorption, indicating the tendency of the NS towards a more disordered system.⁴³ The slight decrease in percentage crystallinity of the NS on adsorption can be the result of an increase in randomness or disorder in the crystal lattice of cellulose.⁴³

Adsorption study

Effect of pH

Many studies suggest that pH is an important factor in the biosorption process,⁴⁴⁻⁴⁵ variations in pH could change the characteristics and availability of dye in solution, as well as the chemical status of the functional groups

responsible for biosorption. Some experiments were therefore performed at 45 °C with 70 mg/L dye solutions to study the MB adsorption on NS as a function of solution pH. The plot of dye adsorption capacity (mg/g) versus pH is shown in Figure 3. It is observed from the graph that maximum adsorption by the NS was observed at pH 6. A decrease in adsorption at pH > 6.0 is due to precipitation of insoluble MB on the available binding sites on the adsorbent surface. Similar results have been reported for MB adsorption using other adsorbents.⁴⁶

Effect of adsorbent dose

The effect of adsorbent dose on the adsorbed amount of MB dye was studied at 45 °C and pH of 6, by varying the adsorbent amounts from 0.2 to 8 g/L, at an initial concentration of dye fixed at 70 mg/L. The analysis showed that the adsorption of MB dye increased as the adsorbent dosage increased from 0.2 to 8 g/L due to the increasing availability of surface sites on the adsorbent for the adsorbed species. A significant increase in adsorption capacity was observed when the dose was increased from 0.2 to 4 g/L, any addition of the adsorbent beyond this dose did not result in any significant change in the adsorption capacity. These results clearly indicated that the NS dosages must be fixed at 4 g/L (Fig. 4), which is the dosage corresponding to the minimum amount of adsorbent that led to constant MB removal for the entire experiments. Similar results were previously reported by other researchers.^{19,46-48}

Effect of contact time

The removal MB dye was assessed as a function of contact time at pH 6, 4 g/L adsorbent and an initial concentration of dye fixed at 70 mg/L. The plot in Figure 5 reveals that the amount of MB adsorbed increases rapidly at the beginning of the adsorption process. This is probably due to the large available surface area of the NS adsorbent, with free adsorption sites. As the surface adsorption sites become occupied, the uptake is controlled by the rate at which the

adsorbate is transported from the exterior to the interior sites of the adsorbent particles. The adsorption capacity of MB increases with the

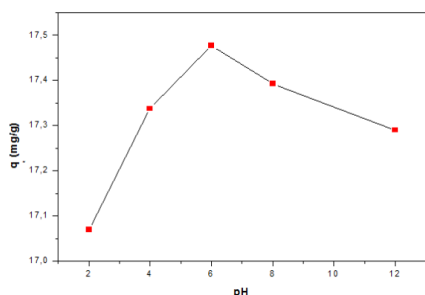


Figure 3: Effect of pH on adsorption of MB dye onto NS adsorbent: adsorbent dose = 1 g/L, V = 250 mL, T = 45 °C, C₀ = 70 mg/L, and contact time = 60 min

contact time and then stabilizes, reaching equilibrium in 20 min. The same phenomenon was observed for other materials.^{46,49}

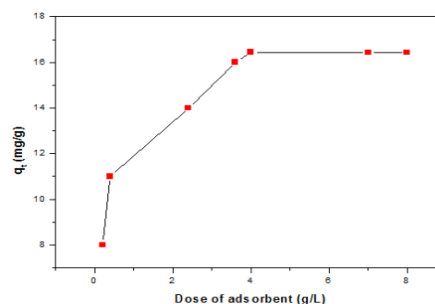


Figure 4: Effect of adsorbent dosage on MB adsorption onto NS adsorbent: V = 250 mL, T = 45 °C, C₀ = 70 mg/L, pH 6, contact time = 60 min

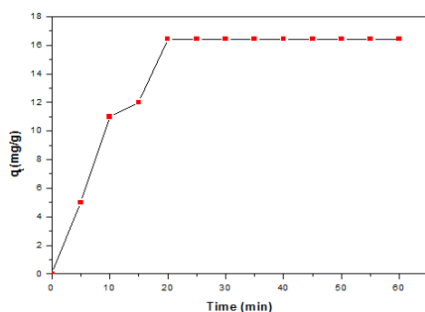


Figure 5: Effect of contact time on MB dye removal onto NS adsorbent: pH 6, 4 g/L adsorbent, C₀ = 70 mg/L, V = 250 mL

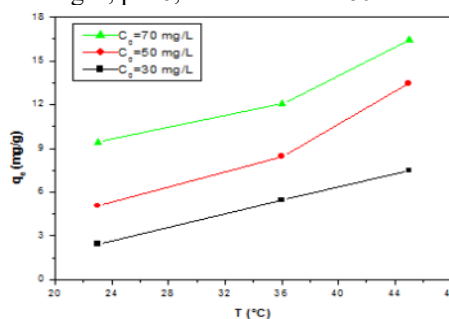


Figure 6: Effect of temperature on adsorption capacity of NS adsorbent for MB dye: pH 6, 4 g/L adsorbent, and V = 250 mL

Effect of initial dye concentration on temperature dependent adsorption

The initial dye concentration provides an important driving force to overcome all mass transfer limitations of dye between the aqueous and solid phases. Therefore, a higher initial MB concentration will enhance the adsorption process. Figure 6 shows the effect of initial MB concentration on the equilibrium adsorption capacity (q_e) of MB on NS at different temperatures. It was clear to see that the q_e values increase with the increase in the initial MB concentrations and with the solution temperature. The maximum equilibrium (q_e) values were determined as 9.43, 12.05 and 16.44 mg/g for 70 mg/L initial MB concentration at 23 °C, 35 °C and 45 °C, respectively. Similar findings have been reported for other adsorbent systems.^{19,46} The adsorption capacity for the system (MB/NS) increases with increasing temperature from 23° to 45 °C. The best removal efficiency (16.44 mg/g

and 93.943%) was obtained at a temperature of 45 °C.

Adsorption isotherms

The study of isotherm models allows describing the interaction and the affinity between solutes and adsorbents, allowing understanding of the adsorption mechanisms and surface properties. The four most common models were used in the present work: the Langmuir, Freundlich, Temkin and Elovich models. The adsorption data for the Langmuir, Freundlich, Temkin and Elovich isotherms are shown in Figure 7 (a-d). Table 4 summarizes the constants of the Langmuir, Freundlich, Temkin and Elovich isotherms, obtained from the slope and the interception of the plots of each isotherm at different temperatures. The values of R² exceed 0.9 for the four models, suggesting that the four models are close to the experimental results.

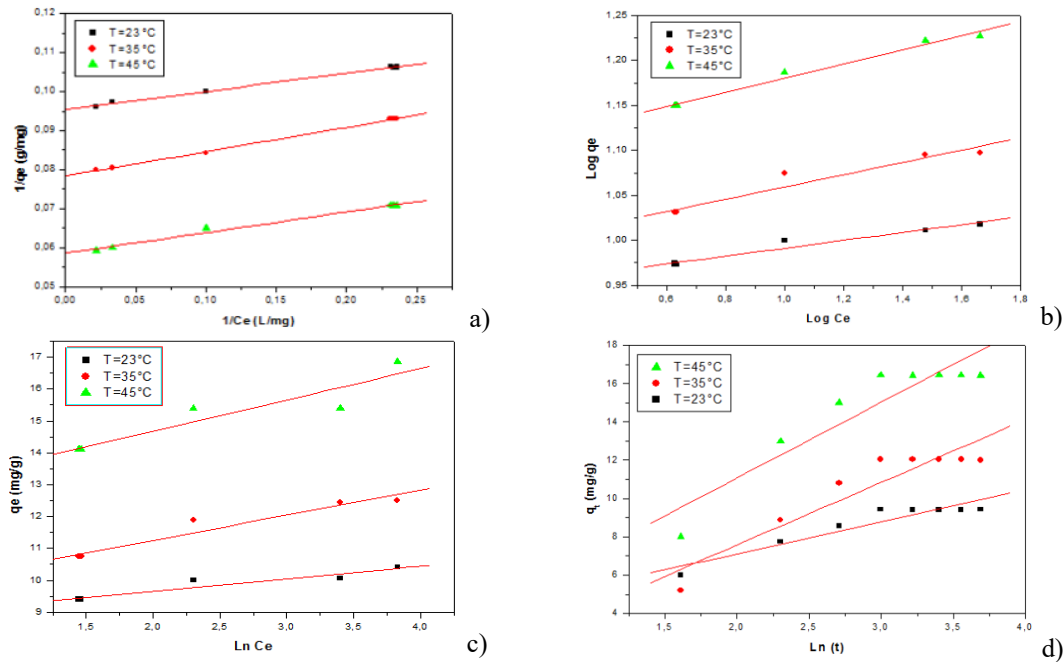


Figure 7: Linearization of Langmuir (a), Freundlich (b), Temkin (c) and Elovich (d) equations for adsorption of MB dye onto NS (pH 6, $C_0 = 70$ mg/L, $V = 250$ mL and 4 g/L adsorbent)

Table 4
Parameters of different adsorption models for the system MB/NS

Isotherm model	Parameter	Temperature (°C)		
		23	35	45
Freundlich	q_{cal} (mg/g)	1.174	3.225	3.706
	$K_F(\text{mg/L})(\text{L/g})^{1/n}$	1.045	2.694	3.007
	$1/n_F$	0.044	0.068	0.079
	R^2	0.980	0.972	0.993
	RMSE	1.79399741	0.42455369	0.56105836
	χ^2	5.97832452	0.31752693	0.49220213
	SSE	0.57307145	0.1356187	0.17922352
Langmuir	$q_{m,exp}$ (mg/g)	9.43	12.05	16.44
	$q_{m,cal}$ (mg/g)	10.482	12.762	17.074
	K_L (L/g)	2.062	1.257	1.107
	R^2	0.998	0.999	0.995
	R_L	0.0159	0.0160	0.0127
	RMSE	0.98578287	1.85019659	2.76140469
	SSE	0.31489679	0.59102362	0.88209837
Temkin	q_m (mg/g)	2.991	11.765	15.314
	K_T (L/g)	536260.0875	199818.769	475274.144
	B_T (J/mol)	6220.946	3232.853	2713.814
	R^2	0.963	0.974	0.941
	RMSE	9.88225098	1.00677489	1.39184721
	χ^2	19.5434119	0.17568008	0.2467959
	SSE	3.49390334	0.35594868	0.4920923
Elovich	q_m (mg/g)	10.613	14.948	10.261
	α_{El} (mg/(g.min))	16.051	4.488	8.834
	β_{El} (g/mg)	0.599	0.306	0.253
	R^2	0.946	0.934	0.927
	RMSE	2.6507356	5.61156727	3.82759465
	χ^2	5.2504581	24.7103197	5.03569634
	SSE	0.84674643	1.79254941	1.22268026

Table 5
Adsorption capacities of various adsorbents for MB dye

Adsorbents	q_{\max} (mg/g)	pH	Ref.
Yellow passion fruit	44.70	--	51
Banana peel	20.8	--	52
Sugarcane bagasse	34.20	--	53
Banana and orange peels	31.25	--	50
Sugarcane bagasse	31	12	54
Wheat husk	21.5	5.5	46
Wheat straw	86.45	6	19
Raw <i>Luffa cylindrica</i>	49.46	10	49
Nut shells	16.44	6	This study

From Table 4, the values of $1/n_F$ were found to be less than 1. The values of R^2 for the Freundlich model (0.980, 0.972 and 0.993, at 23°, 35° and 45 °C, respectively) were high, indicating that this model can be used to characterize the equilibrium adsorption. However, the Freundlich model was not the most suitable one in this study. The Langmuir model provided the best fitting to the isotherm data at various temperatures, with the highest R^2 values, compared to the Elovich, Temkin and Freundlich models. The maximum adsorption capacities (q_m) of NS for MB dye were 10.482, 12.762, and 17.074 mg/g at 23, 35, and 45 °C, respectively. Similar results have been reported by other researchers for wheat husk,⁴⁷ as well as banana and orange peels.⁵⁰

The R_L values were found to be less than 1 and greater than 0 for all experiments carried out at different initial concentrations and temperatures (Table 4). Thus, the NS seems to have good affinity towards MB, and its adsorption capacity increased with rising temperature.

The theoretical parameters of adsorption isotherms, along with the regression coefficients, RMSE, χ^2 and SSE, are listed in Table 4. The equilibrium data fit well to the Langmuir model, with high correlation coefficients. Such coefficients are indicative of monolayer coverage of the MB at the outer surface of the NS particles, and with maximum adsorption capacity (Table 4). The results of Table 4 also show that an increase in temperature from 23° to 45 °C promoted an increase in the adsorption capacity. The Langmuir isotherm model exhibits higher RMSE and SSE values than those of Freundlich.

Table 5 provides a comparison between the experimental results of MB adsorption on NS in this study with those reported by other studies in the literature using various lignocellulosic materials. The data reveal that the adsorbent used in this work (NS) has an acceptable potential for

removing MB dye from water, with a maximum adsorption capacity of 16.44 mg/g.

Kinetics of dye adsorption onto NS adsorbent

The kinetic parameters for adsorption of MB dye presented in Table 6 were calculated from the plots of $\log(q_e - q_t)$ vs t (Fig. 8 a) and the plots of t/q_t vs t (Fig. 8 b). For the studied system (MB/NS), the adsorption mechanism can rely on diffusion in the mesopores or macropores, and, in the absence of micropores, the system tends towards equilibrium. The values of the diffusion rate constants (K_{diff}) are calculated from the graphical representation of the linearized Equation (16).

According to Figure 8 (c), the curves (linear) do not pass through the origin. This shows the dual nature of the adsorption phenomenon. The intercept is due to the presence of an external resistance transfer material, which gives the thickness of the boundary layer.

The results in Table 6 show that the second-order rate constant k_2 decreased with increasing concentrations. The correlation coefficients for the second-order kinetic model were between 0.982 and 0.997. Moreover, the experimental q_e (exp) values agree well with the calculated ones. On the other hand, the correlation coefficients for the pseudo-first-order kinetics ($0.975 < R_2 < 0.995$) were lower than those of the pseudo-second-order one. Furthermore, the values of k_1 obtained from the former had no obvious trend of rise or fall with an increase in concentration. Similar results have been reported by Henini *et al.*⁵⁵ These results indicate that the adsorption system of Methylene blue dye obeyed the pseudo-second-order kinetic model. The pseudo-first-order and pseudo-second-order kinetic models could not identify the diffusion mechanism.

We observe that the diffusion rate constants increase in the same direction as the initial

concentration of MB (Table 6). Indeed for initial dye concentrations between 30 and 70 mg/L, the

values of K_{dif} vary from 1.694 to 3.584 mg/(g min^{1/2}) for the MB/NS system.

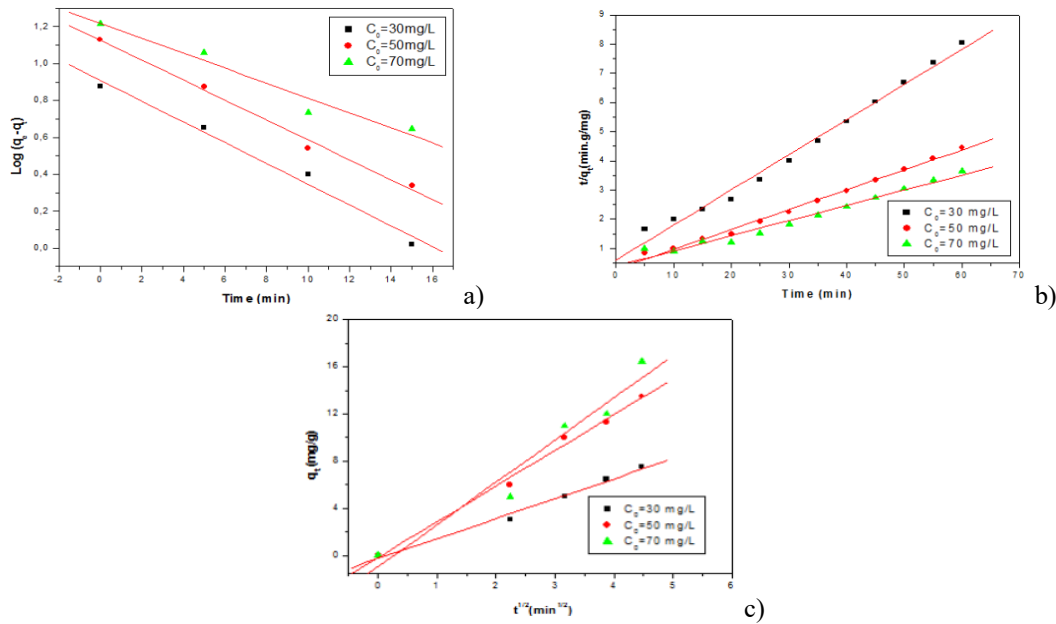


Figure 8: Linearization of pseudo-first-order (a), pseudo-second-order (b) and intraparticle diffusion (c) kinetic models for the MB/NS system, at T = 45 °C

Table 6

Pseudo-first-order and pseudo-second-order kinetic parameters for adsorption of MB dye onto NS adsorbent

C_i (mg/L)	$q_{e,exp}$ (mg/g)	Pseudo-first-order model			Pseudo-second-order model			Intraparticle diffusion		
		$q_{e,cal}$ (mg/g)	K_1 (g/mg.min)	R^2	$q_{e,cal}$ (mg/g)	K_2 (g/mg.min)	R^2	K_{dif} (mg/g.min ^{1/2})	C	R^2
30	7.5	8.118	0.130	0.992	8.302	0.024	0.994	1.694	-0.266	0.994
50	13.48	13.391	0.125	0.996	14.704	0.016	0.997	3.027	-0.163	0.996
70	16.44	16.542	0.093	0.978	19.246	0.007	0.987	3.584	-0.964	0.975

Adsorption thermodynamics

The values of ΔH° and ΔS° can be determined from the slope and the intercept of the plot between $\ln(K_L)$ vs $(1/T)$ (Fig. 9). The ΔG° values were calculated using Equation (18). The values of ΔG° , ΔH° , and ΔS° for the adsorption of MB dye onto NS adsorbent at different temperatures (23°, 35°, and 45 °C) are given in Table 7.

The negative ΔG° values indicates the feasibility and spontaneous nature of the adsorption process with a high preference of MB dye onto NS adsorbent, the negative ΔH° value (-2.557 kJ/mol) shows that the nature of adsorption is exothermic and the negative value of entropy ΔS° (-0.070 kJ/mol.K) shows the decreased randomness at the solid-liquid interface during the process of elimination MB dye on NS adsorbent.³⁵

The rising temperature promotes mobility of the dye ions, and leads to a swelling effect of the internal structure of the NS adsorbent, which will also allow the dye molecules to penetrate further. Therefore, the adsorption capacity will depend largely on the chemical interaction between the functional groups on the adsorbent surface and the adsorbed molecules (which should increase with increasing temperature). This can be explained by an increase in the rate of diffusion of the adsorbate in the adsorbent pores.⁵⁵ The ΔG° values obtained in this study for MB are <-10 kJ/mol, which indicates that physical adsorption was the predominant mechanism in the sorption process.⁵⁶ Barka *et al.*⁵⁷ have reported that the values of ΔG° for the adsorption of the Methylene blue dye on *Scolymus hispanicus* L. adsorbent were found to be -4.04, -3.20, -3.07, -2.24 and -

1.82 kJ/mol for Methylene blue at 293 to 333 K, respectively. These values are 3.27 times greater

than ΔG° in this study at the temperature $T = 23^\circ$ to 45°C .

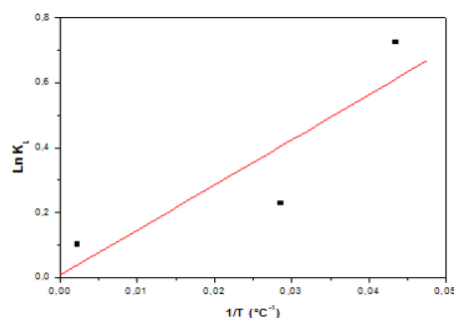


Figure 9: Relationship between Langmuir sorption equilibrium constant and temperature for the MB/NS system at $C_0 = 70 \text{ mg/L}$ dye concentration

Table 7
Thermodynamic parameters for adsorption of MB dye onto NS adsorbent at different temperatures

T (°C)	ΔG° (kJ/mol)	ΔH° (kJ/mol)	ΔS° (kJ/mol K)
23	-1.678		
35	-0.831	-22.557	-0.070
45	-0.126		

CONCLUSION

The results obtained in the present work showed that the biomass derived from locally available agricultural residues (nut shells) can be readily used for the removal of Methylene blue dye from aqueous solutions, with a removal capacity of almost 16.44 mg/g after 20 min. Equilibrium data were fitted to the Langmuir, Freundlich, Temkin and Elovich isotherm models, and the equilibrium data were best described by the Langmuir model ($R^2 = 0.997$). The adsorption kinetics were best described by the pseudo-second-order kinetic model ($R^2 = 0.982$). The thermodynamic parameters for the adsorption of MB onto nut shells were also determined. The negative ΔG° confirms the feasibility and the spontaneous nature of the adsorption process and its physical reaction-based mechanism. Also, the negative ΔS° shows decreased randomness at the solid-solution interface during adsorption, while the negative ΔH° indicates that the adsorption process is exothermic.

ACKNOWLEDGEMENT: The authors are grateful to the colleagues of Plant Chemistry and Chemistry Departments of Chlef University, Algeria, for providing the necessary laboratory data and facilities for this work.

REFERENCES

- 1 M. R. Mafra, I. L. Mafra, D. R. Zuim, É. C. Vasques and M. A. Ferreira, *Braz. J. Chem.*, **30**, 657 (2013), <https://doi.org/10.1590/S0104-66322013000300022>
- 2 A. Fekaoui, G. Henini and Y. Laidani, *Cellulose Chem. Technol.*, **56**, 427 (2022), <https://doi.org/10.35812/cellulosechemtechnol.2022.56.37>
- 3 W. S. Ou, G. Zhang, X. Yuan and P. Su, *J. Water Process. Eng.*, **6**, 120 (2015), <https://doi.org/10.1016/j.jwpe.2015-04-001>
- 4 K. Kavitha and M. M. Senthamilselvi, *Int. J. Curr. Res. Acad. Rev.*, **2**, 270 (2014), <https://doi.org/10.1080/19443994.2013.815687>
- 5 B. K. Nandi, A. Goswami and M. K. Purkait, *Appl. Clay Sci.*, **42**, 583 (2009), <https://doi.org/10.1016/j.clay.2008.03.015>
- 6 A. Khalfaoui, A. H. Meniai and K. Derbal, *Energ. Proc.*, **19**, 286 (2012), <https://doi.org/10.1016/j.egypro.2012.05.208>
- 7 Y. Laidani, G. Henini, S. Hanini and A. Fekaoui, *Iran. J. Chem. Chem. Eng.*, **39**, 131 (2020), <https://doi.org/10.30492/IJCCE.2020.39755>
- 8 J. Sarma, A. Sarma and K. G. Bhattacharyya, *Ind. Eng. Chem. Res.*, **47**, 5433 (2008), <https://doi.org/10.1021/ie071266i>
- 9 I. M. Banat, P. Nigam, D. Singh and R. Marchant, *Bioresour. Technol.*, **58**, 217 (1996), [https://doi.org/10.1016/S0960-8524\(96\)00113-7](https://doi.org/10.1016/S0960-8524(96)00113-7)
- 10 C. Park, Y. Lee, T. Kim, M. Lee, B. Lee *et al.*, *Korean J. Biotechnol. Bioeng.*, **18**, 398 (2003),

<https://koreascience.kr/article/JAKO200311922056760.page>

¹¹ S. F. Adriana, S. O. Leandro and E. F. Mauro, *Desalination*, **249**, 267 (2009), <https://doi.org/10.1016/j.desal.2008.11.017>

¹² B. S. Modesto de Oliveira, *J. Hazard. Mater.*, **174**, 84 (2010), <https://doi.org/10.1016/j.jhazmat.2009.09.020>

¹³ B. H. Hameed and A. A. Ahmed, *J. Hazard. Mater.*, **164**, 870 (2009), <https://doi.org/10.1016/j.jhazmat.2008.08.084>

¹⁴ B. H. Hameed, D. K. Mahmoud and A. L. Ahmad, *J. Hazard. Mater.*, **158**, 499 (2008), <https://doi.org/10.1016/j.jhazmat.2008.01.098>

¹⁵ G. Renmin, S. Jin, Z. Demin, Z. Keding and Z. Guoping, *Bioresour. Technol.*, **99**, 4510 (2007), <https://doi.org/10.1016/j.biortech.2007.08.061>

¹⁶ G. Renmin, D. Yi, L. Mei, Y. Chao, L. Huijun *et al.*, *Dyes Pigments*, **64**, 187 (2005), <https://doi.org/10.1016/j.dyepig.2004.05.005>

¹⁷ M. Davila-Jimenez, M. Elizalde-Gonzalez and V. Hernandez-Montoya, *Bioresour. Technol.*, **100**, 6199 (2009), <https://doi.org/10.1016/j.biortech.2009.06.105>

¹⁸ A. P. Flavio, C. L. Eder, L. P. D. Silvio and C. M. Ana, *J. Hazard. Mater.*, **150**, 703 (2008), <https://doi.org/10.1016/j.jhazmat.2007.05.023>

¹⁹ Y. Laidani, G. Henini, S. Hanini and A. Fekaouni, *Sci. Stud. Res. Chem. Chem. Eng.*, **20**, 609 (2019), <https://pubs.ub.ro/dwnl.php?id=CSCC6201904V04S01A0010>

²⁰ A. R. Khataee, F. Vafaei and M. Jannatkah, *Int. Biodeter. Biodegrad.*, **83**, 33 (2013), <https://doi.org/10.1016/j.ibiod.2013.04.004>

²¹ S. Kalia, A. Kumar and B. S. Kaith, *Adv. Mater. Lett.*, **2**, 17 (2011), <https://doi.org/10.5185/amlett.2010.6130>

²² B. J. Sanghavi, S. M. Mobin, P. Mathur, G. K. Lahiri and A. K. Srivastava, *Biosens. Bioelectron.*, **39**, 124 (2012), <https://doi.org/10.1016/j.bios.2012.07.008>

²³ Y. Laidani, G. Henini, S. Hanini and A. Fekaouni, *J. Env. Sci. Technol.*, **8**, 2544 (2022), <https://www.aljest.net/index.php/aljest/article/download/818/703>

²⁴ T. Lidija Peić, K. Jelena, P. Lato, M. Nikola, K. Jovana *et al.*, *Period. Polytech. Chem. Eng.*, **66**, 629 (2022), <https://doi.org/10.3311/PPch.19783>

²⁵ I. Langmuir, *J. Am. Chem. Soc.*, **40**, 1361 (1918), <https://doi.org/10.1021/ja02242a004>

²⁶ A. Naghizadeh, *J. Water Supply Res. T.*, **64**, 64 (2015), <https://doi.org/10.2166/aqua.2014.022>

²⁷ H. M. F. Freundlich, *Z. Phys. Chem.*, **57A**, 385 (1906), <https://doi.org/10.1515/zpch-1907-5723>

²⁸ H. Nouri, A. Abdedayem, I. Hamidi, S. Souissi Najjar and A. Ouederni, *Cellulose Chem. Technol.*, **55**, 919 (2021), <https://doi.org/10.35812/CelluloseChemTechnol.2021.55.78>

²⁹ G. Henini, Y. Laidani, S. Hanini, A. Fekaouni and K. D. Djallouli, *Sci. Stud. Res. Chem. Chem. Eng.*, **22**,

271 (2021), <https://pubs.ub.ro/dwnl.php?id=CSCC6202103V03S01A0001>

³⁰ O. Baghriche, K. Djebbar and T. Sehili, *Sci. Techn. A*, **27B**, 57 (2008), <https://www.asjp.cerist.dz/en/downArticle/406/0/27/61515>

³¹ M. J. Timken and V. Pyzhev, *Acta Physic. URSS*, **12**, 217 (1940), <https://www.sid.ir/en/Journal/ViewPaper.aspx?ID=312965>

³² W. Saadi, S. Souissi-Najar, M. Othman and A. M. Ouederni, *Cellulose Chem. Technol.*, **57**, 657 (2023), <https://doi.org/10.35812/CelluloseChemTechnol.2023.57.60>

³³ N. Çiriğ Selçuk, Ş. Kubilay, A. Savran and A. Rıza Kul, *OSR J. Appl. Chem.*, **10**, 53 (2017), <http://iosrjournals.org/iosr-jac/papers/vol10-issue5/Version-1/H1005015363.pdf>

³⁴ J. Zhang and R. Stanforth, *Langmuir*, **21**, 2895 (2005), <https://doi.org/10.1021/la047636e>

³⁵ V. Nagarajan, R. Ganesan, S. Govindan and P. Govindaraj, *Period. Polytech. Chem. Eng.*, **65**, 270 (2021), <https://doi.org/10.3311/PPch.17208>

³⁶ W. Alfian, M. Patimah, N. S. Syah Bahar, B. Arini Fousty, P. Neza Rahayu *et al.*, *Period. Polytech. Chem. Eng.*, **67**, 173 (2023), <https://doi.org/10.3311/PPch.21608>

³⁷ G. Crini, *Dyes Pigments*, **77**, 415 (2008), <https://doi.org/10.1016/j.dyepig.2007.07.001>

³⁸ A. Fekaouni, G. Henini and Y. Laidani, *Cellulose Chem. Technol.*, **56**, 427 (2022), <https://doi.org/10.35812/cellulosechemtechnol.2022.56.37>

³⁹ J. R. Weber and J. C. Morris, *J. Sanit. Eng. Div.*, **89**, 31 (1963), <https://doi.org/10.1061/JSEDAI.0000430>

⁴⁰ M. Abbas, S. Kaddour and M. Trari, *J. Ind. Eng. Chem.*, **20**, 745 (2014), <https://doi.org/10.1016/j.jiec.2013.06.030>

⁴¹ V. A. Hidalgo, A. R. Zquez, R. A. Cuevas-Villanueva, L. Marquez-Benavides and R. Cortés-Martinez, *J. Appl. Sci. Environ. Sanit.*, **6**, 447 (2011)

⁴² V. K. Gupta, S. Agarwal, P. Singh and D. Pathania, *Carbohydr. Polym.*, **98**, 121 (2013), <https://doi.org/10.1016/j.carbpol.2013.07.019>

⁴³ B. J. Sanghavi, P. K. Kalambate, S. P. Karna and A. K. Srivastava, *Talanta*, **120**, 1 (2014), <https://doi.org/10.1016/j.talanta.2013.11.077>

⁴⁴ H. Song, Y. Zhou, A. Li and S. Mueller, *Chin. Chem. Lett.*, **03**, 603 (2012), <https://doi.org/10.1016/j.cclet.2012.03.004>

⁴⁵ V. M. Muinde, J. M. Onyari, B. Wamalwa, J. Wabomba and R. M. Nthumbi, *J. Environ. Prot.*, **8**, 215 (2017), <https://doi.org/10.4236/jep.2017.83017>

⁴⁶ Y. Bulut and H. Aydın, *Desalination*, **194**, 259 (2006), <https://doi.org/10.1016/j.desal.2005.10.032>

- ⁴⁷ S. Sadaf and H. N. Bhatti, *J. Taiwan Inst. Chem. Eng.*, **45**, 541 (2014), <https://doi.org/10.1016/j.jtice.2013.05.004>
- ⁴⁸ L. Mouni, D. Merabet, A. Bouzaza and L. Belkhiri, *Desalination*, **276**, 148 (2011), <https://doi.org/10.1016/j.desal.2011.03.038>
- ⁴⁹ N. Boudechiche, H. Mokaddem, Z. Sadaoui and M. Trari, *Int. J. Ind. Chem.*, **7**, 167 (2016), <https://doi.org/10.1007/s40090-015-0066-4>
- ⁵⁰ G. Annadurai, R. S. Juang and D. J. Lee, *J. Hazard. Mater.*, **92**, 263 (2002), [https://doi:10.1016/s0304-3894\(02\)00017-1](https://doi:10.1016/s0304-3894(02)00017-1)
- ⁵¹ F. A. Pavan, E. C. Lima, S. L. P. Dias and A. C. Mazzocato, *J. Hazard. Mater.*, **150**, 703 (2008), <https://doi:10.1016/j.jhazmat.2007.05.023>
- ⁵² R. Gong, S. Zhu, D. Zhang, J. Chen, S. Ni *et al.*, *Desalination*, **230**, 220 (2008), <https://doi.org/10.1016/j.desal.2007.12.002>
- ⁵³ S. P. Raghuvanshi, R. Singh and C. P. Kaushik, *Appl. Ecol. Environ. Res.*, **2**, 35 (2004), <https://doi:10.15666/aeer/03035043>
- ⁵⁴ S. Boumchita, A. Lahrichi, Y. Benjelloun, S. Lairini, V. Nenov *et al.*, *J. Mater. Environ. Sci.*, **7**, 73 (2016)
- ⁵⁵ G. Henini, Y. Laidani and F. Souahi, *Desalin. Water Treat.*, **57**, 1 (2016), <http://dx.doi.org/10.1080/19443994.2014.987169>
- ⁵⁶ B. H. Hameed, A. T. M. Din and A. L. Ahmad, *J. Hazard. Mater.*, **141**, 819 (2007), <https://doi.org/10.1016/j.jhazmat.2006.07.049>
- ⁵⁷ N. Barka, M. Abdennouri and M. El Makhfouk, *J. Taiwan Inst. Chem. Eng.*, **42**, 320 (2011), <https://doi.org/10.1016/j.jtice.2010.07.004>